XLI CILAMCE
XLI Ibero-Latin American Congress on Computational Methods in Engineering
16-19 November, 2020 FOZ DO IGUAÇU PARANÁ - BRAZIL

Bidimensional numerical study of crack propagation on austempered ductile iron

Gustavo von Zeska de França[1], Marco Antônio Luersen[1], Carlos Henrique da Siva[1]

[1]*Dept. of Mechanical Engineer, Federal University of Technology - Parana (UTFPR)*
Rua Deputado Heitor Alencar Furtado, 5000 - Ecoville, 81280-340, Curitiba, Paraná, Brasil
gvzfranca@yahoo.com.br, luersen@utfpr.edu.br, carloshs@utfpr.edu.br

Abstract. The austempered ductile iron (ADI) has a wide range of applications, due to its high mechanical strength, fatigue resistance and wear resistance. ADI is composed by an ausferritic matrix with graphite nodules. The nodule size and amount can be controlled by chemical composition and austenitizing temperature. The nodules have strength lower than the matrix and can act as stress concentrators and influence on crack propagation through changing its trajectory that may generate a protective effect. However, according to the literature, the crack propagation mechanism in ADI is not yet fully understood. In this context, this work presents a bidimensional numerical model that simulates crack propagation based on Paris law for ADI material subjected to cyclic load. The model was implemented in Python language and uses the commercial finite element code ABAQUS. The simulations showed that the presence of a nodule generates a shear load on the crack tip which is the main parameter responsible for changing the crack direction to the nodule itself. Modifications such as increasing nodule size and decreasing nodule distance to crack tip intensify this action. In simulations with two different ADI materials with the same graphite area fraction, increasing the number of nodules causes the crack to have a shorter lifetime until it intercepts a new nodule. Therefore, this suggests that the protective effect of nodules in ADI material may be correlated with the number of intercepted nodules.

Keywords: austempered ductile iron (ADI), fatigue, crack propagation, finite element analysis.

1 Introduction

In the 1940's, the first ductile cast irons (DCIs) were obtainned after the addition of magnesium or cerium to conventional cast iron, as mentioned by Di Cocco and Iacoviello [1]. The austempered ductile iron (ADI), which is formed by an ausferrite matrix with graphite nodules, was introduced in the 1970s. According to Pedro and Dommarco [2], typical applications for this material are gears, cams and followers, mainly due to its good wear resistance. Also, according to Martins *et al.* [3], nowadays, significant developments allow the production of high-resistance ADIs.

According to Lefevre and Hayrynen [4], ADI has a lower relative material cost when compared with cast and forged steels. Furthermore, according to Dias [5], this material has higher mechanical strength, ductility, toughness, fatigue resistance and wear resistance, when compared to other cast irons. And also, as demonstrated by Panneerselvam *et al.* [6], the mechanical properties are influenced by the temperature of the heat treatments, which affect the microstructure of the material.

Another factor that affects the properties of the ADI material is the size and quantity of graphite nodules. Rebasa *et al.* [7] studied several variants of the ADI and DI materials and showed that the amount of graphite nodules can vary from 100 to 1500 nodules/mm². They concluded that, for similar hardness, the rolling contact fatigue (RCF) resistance is higher for samples with high nodules count, which seems to be the mainly parameter responsible for their longer lives.

Dommarco *et al.* [8] demonstrated that the nodule size affects the RCF life, with a strong life increment when the nodule size decreases. According to Gans *et al.* [9], in ADI, the size and number of nodules affects nucleation and propagation stage of cracks, and ADIs with higher amount of nodules have a higher wear resistance.

Greno *et al*. [10] investigated the propagation of fatigue crack in ADI and found that it preferentially intercepts graphite nodules. In addition, the propagation mechanism occurs from small cracks emanating from the nodules and growing towards the principal crack. According to Stokes *et al.* [11], the initiation of the dominant fatigue cracks occurred exclusively in pores, superficial and sub superficial, and in the absence of these defects, the initiation occurs in the graphite nodules. It was found that the growth of the main crack can be deflected due to coalescence with secondary cracks, which may generate a shielding effect.

Problems with ADI have been studied at the microscopic level using finite element analysis (FEA) to understand the effect of the size and the quantity of nodules, as in Gans *et al.* [9]. Suguinoshita *et al.* [12] studied the stress intensity factor at the crack tip using FEA. FEA simulation of fatigue phenomenon intends to determine the component's lifetime. It is necessary to understand the failure mechanisms of the material, among them, the factors that influence on fatigue as the stress intensity factors. In the case of ADI, it is also necessary to understand the influence of the graphite nodules on these factors and, consequently, on the crack propagation speed.

In this work, the influence of the nodule account on a crack propagation due to cyclic loads in an ADI material is studied using a bidimensional FEA model, in which a mixed state of stress occurs (normal stresses and shear stresses) due to the presence of nodules. An iterative crack growth method is implemented to verify the crack development under cyclic load, the crack path and the component's lifetime.

2 Crack propagation routine development

2.1 Methodology

To simulate the crack propagation at ADI material and to verify the stress intensity factors in the crack tip during its growth, a routine that iteratively calculates the crack propagation was developed in Python. In this routine, the user provides the geometry, material, initial crack condition (size, position and angle) parameters, the boundary conditions and the position and size of the nodules. The Python routine read the input data and sends it to the ABAQUS® 6.14 finite element commercial program that run the model. At each iteration the crack is propagated, and its size is increased. The simulation proceed until a stop criterion is reached or the crack reach a nodule.

Some simplifications for the problem were assumed. First, the FEA model was bidimensionaly modeled, and, consequently, the graphite nodules are circumferences which would represent cylinders (not spheres) when extended. In addition, the model is processed in linear elastic fracture mechanics, and therefore the effects of plasticity are ignored and thus the stresses at the crack tip are representative only for the calculation of stress intensity factors. Another simplification for the ADI material is the interface condition between graphite and austenite, which in this case was considered continuous, with only a variation in the mechanical properties between the elements of the two sets of materials.

The ADI properties used in the model were measured by Yan et al. [13] and are described in Tab. 1.

Table 1. ADI mechanical properties

Material	Young's modulus [GPa]	Poisson's ratio
Ausferrite	210	0.290
Graphite nodule	35	0.126

The lifetime calculation is performed by a variant of the Paris Law, proposed by Tanaka [14]. Thus, the influence of crack opening mode II is considered when calculating the crack's lifetime. At the end of each iteration, the routine calculates the crack propagation value, a_i, based on the value of the equivalent stress intensity factor, K_{eff}. Therefore, the number of cycles for each iteration, N_i, is given by

$$N_i = \frac{a_i}{C\left(\Delta K_{eff}\right)^m}, \tag{1}$$

where,

$$\Delta K_{eff} = (\Delta K_I^4 + 8\Delta K_{II}^4)^{\frac{1}{4}}, \tag{2}$$

for the values of C and m the values found by Greno *et al.* [10] of, respectively, 2.891x10^{-11} and 2.74 for ADI material were used.

The total number of cycles, *N*, until the end of the crack propagation simulation is given by the sum of the number of cycles of each iteration, N_i, in all *n* iterations

$$N = \sum_{i=1}^{n} N_i. \tag{3}$$

To calculate the crack propagation direction, θ, in each iteration an ABAQUS subroutine was used. This routine is based on the criterion of maximum tangential stress developed by Erdorgan and Sih [15], where

$$\theta = cos^{-1}\left(\frac{3K_{II}^2 + \sqrt{K_I^4 + 8K_I^2K_{II}^2}}{K_I^2 + 9K_{II}^2}\right), \tag{4}$$

if $K_{II} > 0$ then $\theta < 0$ and if $K_{II} < 0$ then $\theta > 0$.

The routine ends when one of the stop criteria is reached. Which may be, number of iterations, K_{eff} value or if the crack intercepts a nodule.

2.2 Crack propagation study

In this study, the geometry used is based on that used by Silva *et al.* [16] and is adapted to verify the influence of the graphite nodule on crack propagation. The dimensional parameters of the geometry, forces and constraints are shown in Fig. 1.

Three cases with different nodule diameters, d, were studied: 4, 6, and 8 mm. All were positioned at a distance, D, of 8 mm from the beginning of the crack. The angle between the center of the hole and the crack tip with respect to the horizontal is 30°. A crack of initial size, a_0, of 1 mm was positioned, as shown in Fig. 1. Two representative bodies were created to apply force and constraint in the center of the holes. A 700 N force was applied at the upper body and the constraint condition was added to the other.

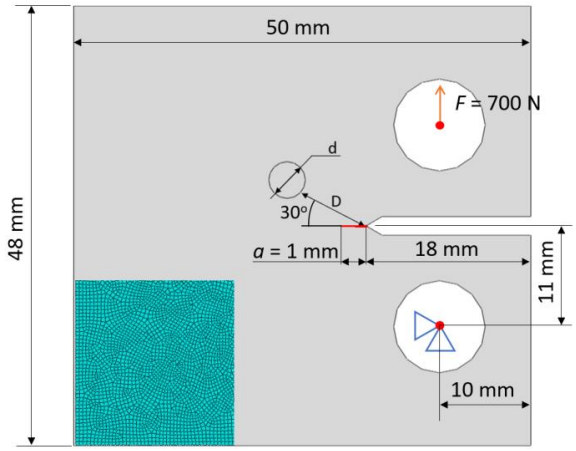

Figure 1. Schematic representation of the stress intensity factor case study and example of mesh used

For this case, a global mesh size of 0.4 mm was generated. The result obtained for the propagation of cracks is shown in Fig. 2. In all cases the crack deviated the horizontal direction to the nodule direction, and in cases (b) and (c) the crack effectively reaches the nodule.

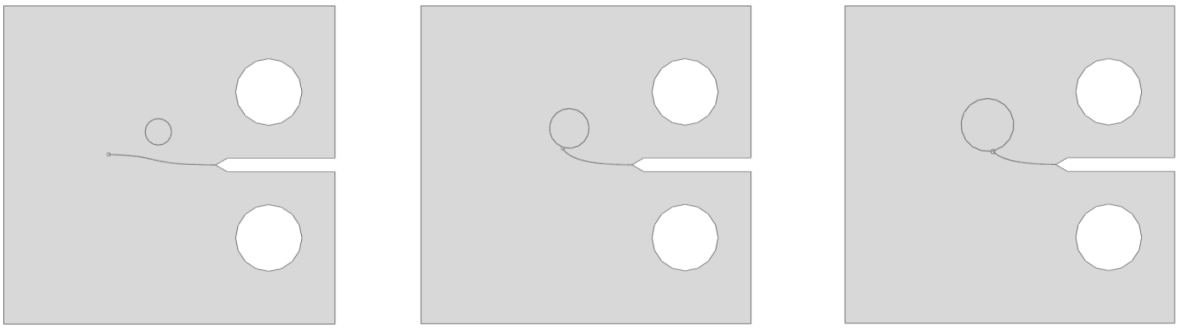

(a) d = 4 mm (b) d = 6 mm (c) d = 8 mm

Figure 2. Crack propagation for cases with different nodule diameters

The variation of the stress intensity factors at the crack tip along its propagation was also verified. Figure 3 shows the values of this factor for mode I (tensile) and for mode II (shear). There is a great difference in the order of magnitude between these two factors, with the factor in mode II being at least 10 times lower than the factor in mode I. Thereby, the equivalent stress intensity factor, Eq. 2, in these cases is approximately equal to the stress intensity factor in mode I.

However, the behavior presented by the stress intensity factor in mode II is still important, as it influences the crack propagation direction, Eq. 4, the positive values of mode II cause the crack to propagate towards the nodule. For Fig 2.(a), with nodule diameter of 4 mm, a negative value for K_{II} appeared after some iterations and the crack deviates from the nodule.

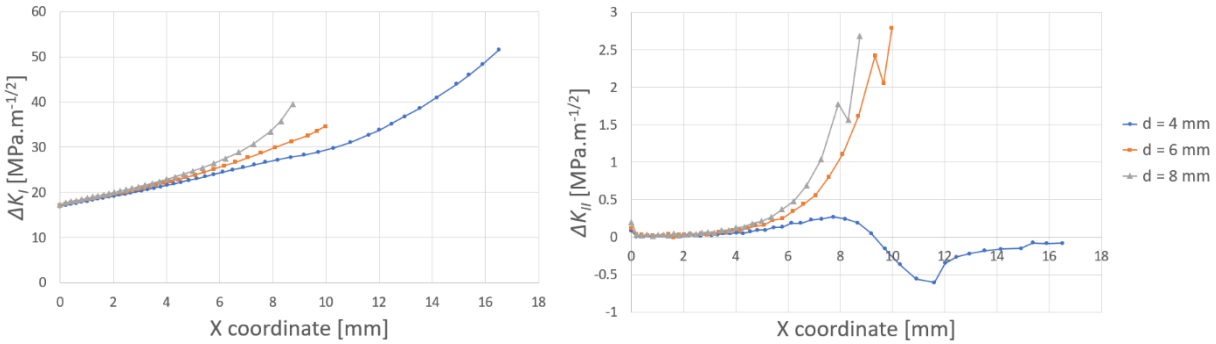

Figure 3. Variation of the stress intensity factor in mode I for different nodule sizes

The crack length, *a*, by the number of cycles, *N*, was also analyzed, Fig. 4 demonstrates the result of this analysis. It is possible to notice that for the same number of cycles, crack propagation is greater for the case with a larger nodule diameter. For this case, the nodule with a larger diameter caused the crack to spread faster and, consequently, has a shorter fatigue life.

A second study in which the distance D from the nodule to the crack tip is varied was also carried out, but to keep the text concise, only its conclusion will be reported. In this study, it was found that the proximity of the crack tip to the nodule increases the value of the stress intensity factor and causes the crack to deviate and grow faster towards the nodule, thus acting in the same way as the increase in the size of the nodule.

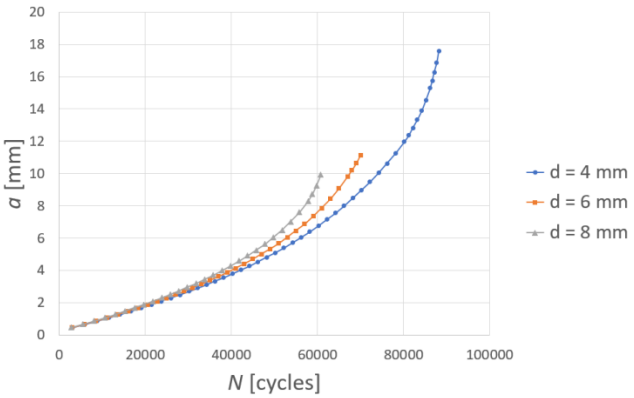

Figure 4. *a* - *N* curves for different nodule sizes.

2.3 Crack propagation on ADI

In this study, a representative area of 1 mm x 1 mm subjected to a cyclic traction in the vertical direction ranging from 0 to 60 MPa of ADI material was analyzed. A central area of 0.8 mm x 0.8 mm was defined to position the graphite nodules, in order to avoid possible edge effects of the load applied on them. In this area, graphite nodules were added according to the characteristics of the materials described by Gans *et al.* [9], Tab. 2. The first node was positioned in the center of the geometry and the others were randomly distributed in the rest of the defined area. The crack, with an initial length of 0.01 mm, was positioned perpendicular to the load and emanating from the central nodule, since, according to Stokes *et al.* [11], this is the way cracks initiate in ADI material in the absence of other defects. Figure 5 shows this case.

Table 2. Characteristics of the ADI materials used by Gans *et al.* [9]

	Graphite fraction area [%]	Nodule count [nodules/mm²]	Nodule diameter [μm]
ADI I	13	196	29.1
ADI II	13	532	17.6

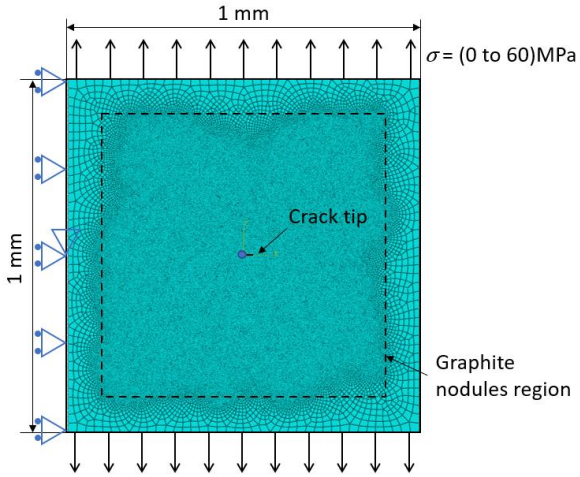

Figure 5. Geometry and boundary conditions for a representative ADI area

The overall size of the element for these cases was set at 0.025 mm, however, in the region of the nodules there is a mesh refinement. For each type of ADI, five cases were simulated with the nodes randomly positioned. An example for each case is shown in Fig. 6, where it is possible to notice the difference in the number of nodules between the two materials due to the difference in the diameter of the nodule.

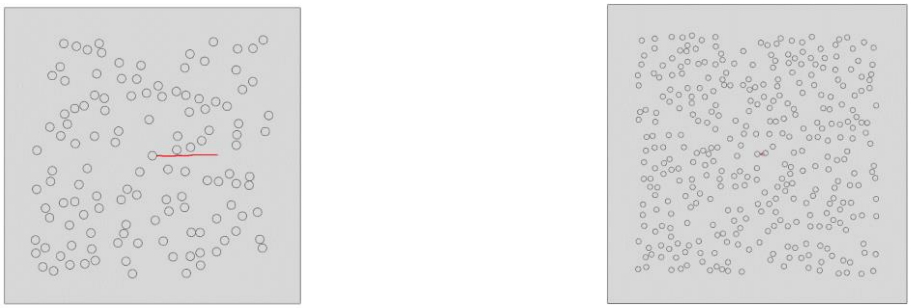

(a) ADI I (b) ADI II

Figure 6. Crack propagation for cases with nodules randomly positioned

When comparing the *a* - *N* curve, Fig. 7, it is possible to verify a large difference between the material ADI I and ADI II. There is a great acceleration in the crack growth for the material with larger nodules. Where, for the same number of cycles, the crack in this material is greater.

Finally, the results also demonstrate that cracks in the material with a greater number of nodules have a trend to propagate a shorter distance until they intercept a new nodule in their path, as shown in Fig. 7. Because the number of nodules is much higher in this material, in addition, the crack has a trend to propagate in the direction of the nodule, depending on the distance and the size of the nodule. The crack had an average spread of 0.071 mm in ADI I material and 0.036 mm in ADI II material, which is practically half the size of the average of ADI I.

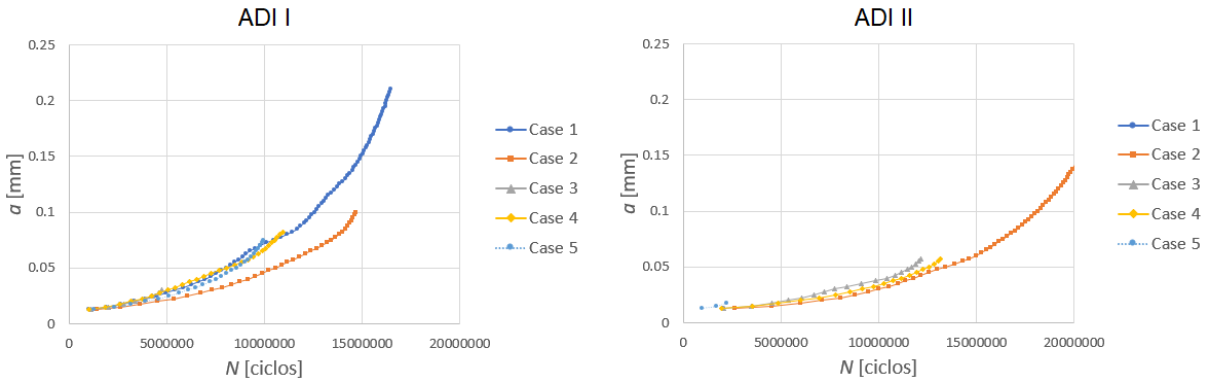

Figure 7. Comparison between *a* – *N* curves of ADI I and ADI II

3 Conclusions

In this work, a numerical-computational routine was implemented in combination with a finite element commercial code to study crack propagation in ADI material. In the cases studied to demonstrate the influence that graphite nodules have on the stress intensity factor and on crack propagation, it was found that the proximity of the crack tip to the nodule and the size of the nodule has a direct influence on the value of the stress intensity factor. It was observed that with the presence of the nodule, under tractive load, the stress intensity factor in mode II is not null and, consequently, there is a perturbation in the crack propagation path. Therefore, the presence of nodules influences mainly the crack propagation direction and can accelerate the crack propagation due to the increase in the stress intensity factor value. However, these points alone still do not justify the high wear resistance of these materials, observed in experimental tests.

The last study, with the distribution of nodules and mechanical properties in order to represent a real structure of the ADI, showed that in materials with nodules of smaller diameter the crack has a trend to intercept a nodule in a smaller number of cycles. Consequently, for the same area fraction of graphics, a crack that propagates on a material with smaller nodules trends to intercept a greater amount of nodules than a crack that propagates in an ADI with a larger nodules. This suggests that the protective effect of the nodules may be correlated with the number of intercepted nodules, as suggested by the studies that correlate the greater wear resistance with the higher number of graphite nodules.

Acknowledgements. The authors would like to thank the Brazilian funding agency CAPES for partially supporting this research.

Authorship statement. The authors hereby confirm that they are the sole liable persons responsible for the authorship of this work, and that all material that has been herein included as part of the present paper is either the property (and authorship) of the authors, or has the permission of the owners to be included here.

References

[1] Di Cocco, V. and Iacoviello, F., "Ductile cast iron: Microstructure influence on the damaging micromechanisms in overload fatigue cracks". *Engineering Failure Analysis*, vol 82, pp. 340–349, 2017.
[2] Pedro, D. I. and Dommarco, R. C., "Rolling contact fatigue resistance of Carbidic Austempered Ductile Iron (CADI)". *Wear*, vol. 418 – 419, pp. 94–101, 2019.
[3] Martins, R.; Seabra, J. and Magalhães, L., "Austempered ductile iron (ADI) gears: Power loss, pitting and micropitting". *Wear*, vol. 264, n. 9 – 10, pp. 838–849, 2008.
[4] Lefevre, J. and Hayrynen, K. L., "Austempered materials for powertrain applications". *Journal of Materials Engineering and Performance*, vol. 22, n. 7, pp. 1914–1922, 2013.
[5] Dias, J. F., "Estudo do comportamento à fadiga em ferro fundido nodular austemperado (ADI) sujeito a carregamento de amplitude variável". PhD Thesis (Doutorado em Engenharia de Estruturas) Universidade Federal de Minas Gerais (UFMG), 2006.
[6] Panneerselvam, S.; Putatunda, S. K.; Gundlach, R. and Boileau, J., "Influence of intercritical austempering on the microstructure and mechanical properties of austempered ductile cast iron (ADI)". *Material Science and Engineering: A*, vol. 694, pp. 72–80, 2017.
[7] Rebasa, N.; Dommarco, R. and Sikora, J., "Wear resistance of high nodule count ductile iron". *Wear*, vol. 253, pp. 855–861, 2002.
[8] Dommarco, R. C.; Jaureguiberry, A. J. and Sikora, J. A., "Rolling contact fatigue resistance of ductile iron with different nodule counts and matrix microstructures". *Wear*, vol. 261, n. 2, pp. 172–179, 2006.
[9] Gans, L. H. A.; Guesser, W. L.; Luersen, M. A. and da Silva, C. H., "Numerical analysis of the influence of graphite nodule size on the pitting resistance of austepered ductile iron gears". *Advanced Materials Research*, vol. 1120–1121, pp. 763–772, 2015.
[10] Greno, G. L.; Otegui, J. L. and Boeri, R. E., "Mechanisms of fatigue crack growth in austempered ductile iron". *International Journal of Fatigue*, vol. 21, n. 1, pp. 35–43, 1999.
[11] Stokes, B.; Gao, N. and Reed, P. A. S., "Effects of graphite nodules on crack growth behaviour of austempered ductile iron". *Materials Science and Engineering: A*, vol. 445 – 446, pp. 374–385, 2007.
[12] Suguinoshita, G.; da Silva, C. H. and Luersen, M. A., "A finite element study of the influence of graphite nodule characteristics on a subsurface crack in a ductile cast iron matrix under a contact load". *Computer Modeling in Engineering & Sciences*, vol. 117, n.(1, pp. 59–71, 2018.
[13] Yan, W.; Pun, C. L.; Wu, Z. and Simon, G. P., "Some issues on nanoindentation method to measure the elastic modulus of particles in composites". *Composites: Part B*, vol. 42, pp. 2093–2097, 2011.
[14] Tanaka, K., "Fatigue crack propagation from a crack inclined to the cyclic tensile axis". *Engineering Fracture Mechanics*, vol. 6, n.3, pp. 493–498, 1974.
[15] Erdogan, F. and Sih, G. C., "On the crack extension in plates under plane loading and transverse shear". *Journal of Basic Engineering*, vol. 85, n. 4, pp. 519–525, 1963.
[16] Silva, A. L. L.; de Jesus, A. M. P.; Xavier, J.; Correia, J. A. F. O. and Fernandes, A.A., "Combined analytical-numerical methodologies for the evaluation of mixed-mode (I + II) fatigue crack growth rates in structural steels". *Engineering Fracture Mechanics*, vol. 185, pp. 124–138, 2017.